The mechanism of chlorogenic acid inhibits lipid oxidation: An investigation using multi-spectroscopic methods and molecular docking

The mechanism of chlorogenic acid inhibits lipid oxidation: An investigation using multi-spectroscopic methods and molecular docking

Qiongju Cao [a]; Yuan Huang [a, b]; Quan-Fei Zhu [c]; Mingwei Song [d]; Shanbai Xiong [a, b]; Anne Manyande [e]; Hongying Du [a, b*]

[a] College of Food Science and Technology, Huazhong Agricultural University, Wuhan, Hubei 430070, P.R. China;

[b] National R & D Branch Center for Conventional Freshwater Fish Processing, Wuhan, Hubei 430070, P.R. China;

[c] Department of Chemistry, Wuhan University, Wuhan, 430072, P.R. China

[d] College of Resources and Environment, Huazhong Agricultural University, Wuhan, 430070, P. R. China

[e] School of Human and Social Sciences, University of West London, London, UK;

*: **Corresponding author**

Hongying Du, Email: hydu@mail.hzau.edu.cn, Tel: +86-27-87283007

Abstract: Endogenous lipase and lipoxygenase play important roles in accelerating lipid oxidation. Polyphenols are a series of commonly used chemicals for preserving fish and seafood products, due to their positive inhibitory effects on lipid oxidation. However, the mechanism involved is still unknown. The inhibitory effects of chlorogenic acid (CGA) on lipase and lipoxygenase were investigated and explored with multi- spectroscopic and molecular docking approaches. Results showed that CGA could inhibit the activities of lipase and lipoxygenase with concentration increased in a highly dose-dependent manner. CGA quenched intrinsic fluorescence intensities of enzymes by static quenching and binding with CGA which led to changes in 3D structures of enzymes. Results of the molecular docking confirmed binding modes, binding sites and major interaction forces between CGA and enzymes, which reduced the corresponding activity. Thus, this study could provide basic mechanisms of the inhibitory effects of polyphenols on lipid oxidation during food preservation.

Keywords: Chlorogenic acid; Lipase; Lipoxygenase; Spectroscopy analysis; Molecular docking;

1 Introduction

Lipase (triacylglycerol acylhydrolases, EC 3.1.1.3) belongs to carboxylesterases and widely exists in animals and plants. It catalyzes the hydrolysis of triglycerides, which contain long-chain fatty acids at sn-2 and sn-1 positions, to free fatty acid and glycerol at the lipid-water interface (Cherif & Gargouri, 2009). Hydrolysis products can further be oxidized by lipoxygenase and free radicals. Lipoxygenase (LOX, EC 1.13.11.12), a class of protein which contains non-heme iron, specifically catalyzes polyunsaturated fatty acids and fatty acid esters with a 1,4-*cis*, *cis* pentadiene structure into hydroperoxide (Andreou, et al., 2010). The catalytic site of LOX is composed of metal ion and amino acid residues. LOX oxidizes unsaturated fatty acids and esters into hydro peroxide derivatives (Nikpour, et al., 2013). Previous studies showed that lipase and LOX affect important physiological reactions which are involved in the pathogenesis of various diseases in humans (Schreiber, et al., 2019).

Enzymatic reactions are not only closely related to human diseases, but are also associated with lipid oxidation of fish and fish products during transportation, processing and storage. Oxidizing reaction in the muscle tissue leads to undesirable changes and quality deterioration, such as production of off-odor, rancid flavors, and changes in color and texture (Chauhan, et al., 2018). The increasing content of carbonyl compounds and free fatty acid, which are the main products of enzymatic reactions, influence the flavor of meat (Huang & Ahn, 2019). When the concentration of compounds like hexanal, pentanal, 2, 6-nonadienal and 1-octen-3-one, plus 2, 3-octanedione is high enough, it will produce unpleasant odor. Furthermore, when oxidative products of lipid accelerate protein oxidation, some functions for instance, water holding capacity and protein extractability decline with the oxidation proceeding. These lead to the deterioration of protein functional properties during food processing and preservation, for example, loss of moisture, decrease in hardness and emulsion capacity (Utrera, et al., 2015). Therefore, the inhibition of endogenous enzyme-induced lipid oxidation has become more and more important to fish and fish products.

Polyphenols, as one of the representative natural antioxidants, have been shown to perform well in inhibiting lipid oxidation during fish processing and preservation. For instance, the combination of tea polyphenols and vacuum packaging treatment used in weever (*Micropterus salmoides*) storage, presented better quality enhancement effects and good quality control which extended the conrresponding shelf life at 0 ºC and 4 ºC (Ju, et al., 2018). Glazing treatment with rosemary (*Rosmarinus officinalis*) extract displayed the best performance in controlling protein and lipid changes of mud shrimp (*Solenocera melantho*) stored at -20 ºC (Shi, et al., 2019). Furthermore, phenolic compounds such as caffeic acid, coumaric acid, capsaicin, quercetin, epigallocatechingallate (EGCG) showed inhibitory effects on pancreatic lipase *in vitro* (Martinez-Gonzalez, et al., 2017). Chlorogenic acid (CGA), the ester of caffeic acid and quinic acid, is a type of polyphenol widely present in natural plants. CGA exhibits various biological properties which include antioxidant, antibacterial, anti- inflammation (Karar, et al., 2016) and anti-glycation (Gugliucci, et al., 2009). Therefore, the absorption of CGA might induce biological effects in the whole body system, such as protection against cardiovascular disease; and the inhibition of the formation of mutagenic and carcinogenic N-nitroso compounds (Olthof, et al., 2001). Besides the healthy and various biological effects, it has been demonstrated that it is effective in food preservation, for example peach storage (Jiao, et al., 2019) and raw refrigerated chicken (Sun, et al., 2020). In recent years, research on CGA has focused on the preservation of aquatic products. For example, CGA-gelatin combined with partial freezing effectively delayed the decay of sword prawn (*Parapenaeopsis hardwickii*) (Ge, et al., 2020). However, there are very few studies that have demonstrated the application of grass carp preservation in the field. Recently, we found that CGA showed good efficiency in inhibiting lipid oxidation of grass carp muscle during chilled storage (Cao, et al., 2019). However, the mechanism of action of CGA and mode of inhibition of lipid oxidation during fish preservation is still not yet clear. Thus, the interactions between CGA and lipase/lipoxygenase are important

for understanding the mechanism of the application of CGA on grass carp preservation.

In this study, the interactions of CGA with endogenous enzymes extracted from grass carp muscle were investigated using enzyme activity inhibition assay, intrinsic fluorescence quenching measurement, secondary structure determination and Fourier transform- infrared spectroscopy (FT-IR) measurement. Moreover, the information of binding modes and binding sites of CGA on lipase and LOX were separately explored utilizing the molecular docking method. We aimed to explain or give some insights into the inhibitory mechanism of CGA on lipid oxidation during fish preservation.

2 Materials and methods

2.1 Materials

CGA was purchased from Melonepharma (Dalian, Liaoning, China) while 4-nitrophenyl butyrate (4-NPB) was obtained from Sigma–Aldrich Chemical Co (St. Loius, MO, USA) and linoleic acid from Aladdin (Shanghai, China). Protein loading buffer (5×) was purchased from Kerui (Wuhan, Hubei, China). All reagents and chemicals used were of analytical grade.

2.2 Fish sample preparation

All procedures were approved by the Animal Care and Use Committee of Huazhong Agricultural University and performed in accordance with the Guidelines for Care and Use of Laboratory Animals of Huazhong Agricultural University. Fresh grass carp (3.5±0.5 kg, n=10) were purchased from a local fish market (Wuhan, Hubei, China). The sampled fish were anaesthetized using MS‐222 (100 mg/L, 3-Aminobenzoic acid ethyl ester methanesulfonate, Shanghai yuanye Bio-Technology Co., Ltd, Shanghai, P.R. China) and were unconscious before slaughter. Then the fish were immediately decapitated and gutted, and the red muscle under the skin was removed, and the white muscle collected, weighed and mixed for further study.

98 **2.3 Extraction of endogenous enzymes**

99 The extraction of lipase was carried out following the Smichi method (Smichi, et al., 2013). The fish
100 muscle sample was homogenized in ten times volume (1:10, *w*/*v*) 25mM Tris-HCl buffer (pH=8.0, 4 ºC,
101 150 mM NaCl, 2 mM benzamidine) with a blender (Y-QSJ1, Oidire, German) for 3×10 s (4000 rpm). Then
102 the mixture was stirred with a magnetic bar (Thermo, Massachusetts, USA) for 45 min (4 ºC), and
103 centrifuged for 20min (4 ºC, 10000×*g*). The supernatant was collected and ammonium sulphate added (40%
104 of the supernatant weight). The mixture was stirred for 45 min at 4 ºC, and centrifuged at 10000×*g* for 15
105 min. The supernatant was collected and ammonium sulphate added to 60% saturation. Lastly, the solution
106 was stirred and centrifuged using the same procedure, and the sediment (lipase) was collected into a dialysis
107 bag for desalting with former Tris-HCl buffer for 24h, and the buffer was changed every 6h.

108 The lipoxygenase (LOX) was extracted according to a former method (Gata, et al., 1996). Generally,
109 the fish muscle sample was homogenized in five times volume (*v*/*m*: 5:1) phosphate buffer (pH=7.4, 50mM,
110 1mM Dithiothreitol, 1 mM Ethylenediaminetetraacetic acid (EDTA)) with a blender (4000 rpm, 4×10s).
111 The mixture was stirred with a magnetic bar at 4 ºC for 30min, and further centrifuged (4 ºC, 10000×g) for
112 20min. The supernatant was collected and filtrated through a gauze to obtain a crude enzyme solution. To
113 the crude solution was added ammonium sulphate to 20% saturation, stirred for 45min (4 ºC) and then
114 centrifuged for 15 min (4 ºC, 10000×*g*). The supernatant was collected and ammonium sulphate added to
115 40% saturation, stirred and centrifuged with former parameters. Finally, the sediment (LOX) was collected
116 and dialyzed following the same extraction procedure of lipase.

117 **2.4 SDS-PAGE (Sodium dodecyl sulfate - polyacrylamide gel electrophoresis)**

118 The protein content in a sample was determined with the Lowry method (Lowry, et al., 1951), and the
119 molecular weight of the endogenous enzyme was determined using SDS-PAGE analysis (n=4). The detailed

120 procedure of the SDS-PAGE was describe in our previous study (Huo, et al., 2016) with slight modification
121 of the solution. The best concentration of separating gel was set to 10%. After electrophoresis, the gel was
122 stained with ~0.1% (*w*/*v*, 0.29g in 250 ml) Coomassie blue R-250, dissolved with the solution (250 ml) of
123 8% (*v*/*v*) acetic acid and 25% (*v*/*v*) ethanol (95%); and destained overnight in 8% (*v*/*v*) acetic acid and 25%
124 (*v*/*v*) ethanol (95%). The markers of proteins (10 to 250 kDa) were also run in parallel on the same gel to
125 determine the molecular weights of the protein.

126 **2.5 Enzyme inhibition assay**

127 Lipase activity was determined using the 4-NPB method (n=3) (Kuepethkaew, et al., 2017). The
128 substrate solution was prepared by dissolving 4-NPB in isopropanol. The reaction was carried out by mixing
129 800 μL diluted lipase, 800 μL CGA solution, and 2.0 mL 50 mM Tris-HCl buffer (pH=8.0, containing 0.5 %
130 Tritox X 100, 25mM NaCl). The reaction was initialized with the addition of 400 μL substrate solution, and
131 the mixture reacted at 37 ºC for 15 min. The absorbance was measured with ultraviolet-visible
132 spectrophotometer at 410 nm and one unit of enzyme activity was defined as the enzyme liberated per μmol
133 of p-nitrophenol in 1 minute. There were three types of inhibition experiments performed with different
134 concentrations of solution. For the inhibition ratio, the concentrations of lipase and 4-NPB solution were
135 0.1mg/mL and 3mM, respectively. For the inhibition type experiments, the following concentrations were
136 used: lipase: 0.025, 0.05, 0.1, 0.2, 0.3 mg/mL; CGA: 0, 0.1, 0.2, 0.3 mg/mL; 4-NPB: 3mM. For the inhibition
137 kinetics experiments, the following concentrations were investigated: lipid: 0.1mg/mL; CGA: 0, 0.1, 0.2,
138 0.3 mg/mL; 4-NPB: 1, 2, 3, 4, 5 mmol/L.

139 LOX's activity was measured according to a former method (n=3) (Gata, et al., 1996). The substrate
140 solution of LOX was prepared by dissolving linoleic acid in distilled water (10 mL, 180μL Tween 20) and
141 the pH value was adjusted to 9.0 with 2 M NaOH. Subsequently, 200μL diluted LOX solution was mixed

with 200μL CGA solution and 50 mM citric acid buffer (pH=5.5, 2.4mL), and the mixed solution was incubated for 10 min (25 ℃). Then, 200μL substrate solution was added to initialize the reaction. One minute after the reaction, the absorbance at 234 nm was recorded. One unit of LOX's activity was defined as an increase of absorbance at 234 nm of 0.001 per min under assay condition (Gata, et al., 1996). For the inhibition ratio, the concentrations of LOX and linoleic acid were 0.1 mg/mL and 20 mM, respectively. For the inhibition type experiments, the following concentrations were used: LOX: 0.05, 0.1, 0.2, 0.3, 0.4 mg/mL; CGA: 0, 0.05, 0.1, 0.2 mg/mL; linoleic acid: 15 mM. For the inhibition kinetics experiments, the following concentrations were investigated: LOX: 0.1 mg/mL; CGA: 0, 0.05, 0.1, 0.2 mg/mL; linoleic acid: 5, 10, 15, 20, 25 mmol/L.

2.6 Fluorescence spectra measurements

The detected enzyme solution (0.1mg/mL) contains relative buffer and different concentrations of CGA (0 M to 40.0×10^{-6} M, stepped by 5×10^{-6} M). The fluorescence spectra of the sample (n=3 for every group) were recorded on F-4500 fluorescence spectrometer (Hitachi, Japan) after standing for 30 min to equilibrate, and the fluorescence measurement was performed at three different temperatures (298K, 303K and 310K). The fluorescence intensity was corrected using the following equation:

$$F_{corr} = F_{obs} \times e^{(A_{ex}+A_{em})/2} \quad (1)$$

where F_{cor} and F_{obs} refer to the corrected and observed fluorescence intensities, respectively. A_{ex} and A_{em} represented the absorption of the ligand at excitation and emission wavelengths, respectively.

For the fluorescence quenching measurement, the following parameters were set: excitation wavelength: 280 nm; emission slits: 5 nm; voltage: 400V; scanning rate: 1200 nm/min; and emission spectra: 290 to 450 nm. For synchronous fluorescence spectra, several parameters were changed: the intervals between emission

and excitation wavelength ($\Delta\lambda$): 15 nm and 60 nm; emission spectra: 240 to 310 nm.

2.7 Ultraviolet-visible (UV-VIS) absorption spectra measurements

The detected enzyme solution (0.1 mg/mL) containing relative buffer and different concentrations of CGA (0 to 40×10^{-6} M, stepped by 10×10^{-6} M) were detected with UV-2600 spectrophotometer (UNIC, China) and performed in the range of 230 - 450 nm at room temperature (n=3 for every group) .

2.8 Circular dichroism (CD) spectra measurements

The changes in secondary structures of endogenous enzymes before and after adding CGA were recorded by a Jasco-1500 spectrophotometer (JASCO, Japan) 2.0 mm path length cell at room temperature (n=3 for every group). The constant concentration of enzymes was 0.05mg/mL, CGA concentrations in the complexes were 0, 20.0 and 40.0×10^{-6} M. The CD spectra were recorded from 190 to 250 nm with a scan rate of 200 nm /min, the response time was 2 s. The spectra data were converted to mean ellipticity in deg cm^2 $dmol^{-1}$ to calculate the secondary structure of enzymes.

2.9 Fourier transform infrared (FT-IR) spectroscopy measurements

The FT-IR spectra were recorded by a Nicolet470 FT-IR spectrometer (Nicolet, USA) (n=3 for every group). The detected enzyme solutions (0.1 mg/mL) containing various CGA (0.0, 20.0 and 40.0×10^{-6} mol/L) were lyophilized for measurement, and the KBr disc was prepared and measured by adding KBr with or without samples. The spectra were scanned in the range of 500-4000 cm^{-1} with 64 scans and 4 cm^{-1} resolutions. Background spectrum was recorded before each sample measurement.

2.10 Dynamic light scattering (DLS)

The enzyme solution (0.01 mg/mL) containing relative buffer and different concentrations of CGA (0 to 4×10^{-6} M, stepped by 1×10^{-6} M) was detected by light scattering determined with Zetasizer Nano ZS90 (Malvern, UK). Each measurement was performed with 11 scans and each sample (n=3 for every group)

186 replicated three times.

187 **2.11 Molecular docking**

188 The interaction between CGA and lipase or LOX were simulated using the molecular docking method
189 performed with CDOCKER module available in Discovery Studio 2016 (BIOVIA, USA). The structures of
190 CGA were collected from PubChem (http://pubchem.ncbi.nlm.nih.gov/), and the crystal structures of lipase
191 (Protein Data Bank (PDB) ID: 1ETH) and LOX (PDB ID: 2P0M) were downloaded from PDB
192 (http://www.rcsb.org/).

193 To prepare protein structures, several steps were initially completed in the software, such as the removal
194 of water molecules and addition of hydrogen atoms. The structure of CGA was optimized due to minimized
195 energy. The docking between CGA and proteins was based on CHARMm force field. The top hit value was
196 set to 10, pose cluster radius was set to 0.5, other docking parameters were default if not mentioned. The
197 lipase-CGA and LOX-CGA interactions are illustrated in 3D and 2D diagrams using Discovery Studio (Xu,
198 et al., 2019).

199 **2.12 Statistical analysis**

200 Statistical analysis was performed with SPSS 22.0 (IBM, New York, USA) using one-way ANOVA.
201 Duncan(D) adjustment was used to determine the significant difference between different groups.
202 Significant differences were declared at $p < 0.05$. The results were expressed as means ± SD (standard
203 deviation).

204

205 **3 Results and discussion**

206 **3.1 SDS-PAGE analysis of endogenous enzymes in fish flesh**

207 The purity of enzymes was confirmed by SDS-PAGE, and the results are shown in Fig. 1a. The
208 molecular weights of lipase and LOX were about 36 kDa and 97 kDa, and the results are illustrated in Fig.
209 1a-sample 5 and 1a-sample 3. The molecular weight of LOX is similar to that reported in mackerel (*Scomber*

210 *scombrus*) and ham (Banerjee, 2006), and the molecular weight of lipase was also found in grey mullet and
211 whiteleg shrimp (Smichi, et al., 2013).

212 **3.2 Inhibitory activities and inhibition kinetics for endogenous enzymes**

213 The inhibitory activities of endogenous lipase and LOX in fish flesh were investigated and the results
214 are illustrated in Fig. 1b-1d. For the inhibitory ratio, the inhibition curves under different concentrations of
215 CGA on the activities of endogenous enzymes were constructed (Fig.1b1 and 1b2). Results show that
216 inhibitory ratios of CGA against enzyme activities were increased with the addition of CGA. The IC_{50} values
217 of CGA on lipase and LOX were 0.58 and 0.32 mg/mL, respectively. Results indicate that CGA was an
218 efficient inhibitor for both lipase and LOX and had significantly stronger inhibitory activity for LOX
219 compared with lipase. The kinetic plots of CGA inhibiting lipase and LOX under the same conditions were
220 explored to elucidate the effects (Fig. 1c). As shown in Fig. 1c1 and 1c2, a group of straight lines passed
221 through the origin point, thus both the inhibition processes of CGA on lipase and LOX were reversible (Yu,
222 et al., 2019).

223 For the inhibitory kinetics study, the double reciprocal plot or Lineweaver-Burk plot was employed to
224 analyze the kinetics parameters, Michaelis-Menten constant (K_m) and the maximum velocity (V_m), in the
225 presence of CGA and 4-npb/ linoleic acid (Fig.1d1 and 1d2). For lipase, the addition of CGA increased the
226 K_m value (from 0.93 mg/mL to 2.06 mg/mL), but the V_m (0.01/min) was constant, which indicates that CGA
227 competitively inhibited lipase activity due to binding to the catalytic site of enzymes. The free enzyme
228 inhibition constant (K_i) was 0.23 mg/mL for the lipase inhibition measurement. The competitive inhibition
229 of pancreatic lipase was also reported for compounds extracted from plants such as Ligupurpuroside B and
230 tea saponin (Ying, et al., 2018). For LOX, the increasing value of K_m (from 4.16 mg/mL to 5.03 mg/mL)
231 and decreasing value of V_m (from 0.22/min to 0.16/min) indicates that there is mixed type inhibition. Results

232 imply that CGA might bind to LOX and linoleic acid-LOX complex simultaneously (Yu, et al., 2019).
233 Similar results were also reported in the inhibition of mackerel (*Scomber scombrus*) muscle lipoxygenase
234 by green tea polyphenols (Sreeparna, 2006). Finally, the K_i and the bound enzyme inhibition constant (K_{is})
235 were found to be 0.32 mg/mL and 0.57 mg/mL.

236 **3.3 Fluorescence quenching**

237 The effect of CGA on tertiary structures of enzymes could be evaluated by the intrinsic fluorescence,
238 which indicates the interactions of CGA and amino acids in aromatic ring structures in proteins including
239 tryptophan (Trp), tyrosine (Tyr) and phenylalanine (Phe) (Cysewski, 2008). The fluorescence emission
240 spectra of lipase and LOX in the presence of different concentrations of CGA at 298K were studied (Fig.
241 2a1 and 2a2). The fluorescence intensities of enzymes were decreased following an increase in CGA and
242 were decreased 44.35% and 60.20% for lipase and LOX respectively. The quenching effects of intrinsic
243 fluorescence indicate the existence of interactions between enzymes and CGA. The intrinsic fluorescence
244 of LOX is easily quenched with CGA, which means there are more opportunities for interaction between
245 CGA and LOX. The results could explain the stronger inhibition of LOX with CGA than with lipase. As
246 shown in Fig. 2a2, the slight redshift in maximum emission wavelength of LOX suggest the increasing
247 hydrophilic microenvironment around fluorophore and amino acid residues after binding with CGA (Xiong,
248 et al., 2016). Furthermore, similar variation tendency was obtained for the fluorescence spectra of lipase
249 and LOX in the presence of different concentrations of CGA at 304K and 310K (Data not shown).

250 **3.3.1 Mechanism of fluorescence quenching**

251 The quenching mechanism by small molecule quenchers can be classified as static quenching and
252 dynamic quenching, which can be analyzed using the Stern-Volmer equation (Lakowicz, Joseph, 2006):

253 $$\frac{F_0}{F} = 1 + K_{SV}[Q] = 1 + K_q\tau_0[Q] \quad (2)$$

where F_0 and F are the fluorescence intensities of the complex without and with CGA, respectively; K_{sv} is the quenching constant; K_q is the quenching rate constant of the biomolecule; *[Q]* is the concentration of CGA and τ_0 is the average life time of molecules in the absence of the quencher (the value is approximately 10^{-8} s^{-1}).

As shown in Fig. 2b1 and Fig. 2b2, the Stern-Volmer curves show good liner relationships. The K_{sv} and Kq for the interactions between CGA and enzymes at different temperatures were collected in Table 1. The Kq of lipase and LOX were 2.11×10^{12} L/mol·s and 3.94×10^{12} L/mol·s at 298K respectively, which were much higher than the maximum dispersion collision quenching constant (2.00×10^{10} L/mol·s). The results suggest that the formation of complexes between CGA and endogenous enzymes and the quenching types of lipase and LOX caused by CGA belong to static quenching. Besides, the K_{sv} values of both interaction systems decreased with increasing temperature, which also presented the characteristics of fluorescence static quenching.

The binding constant (K_a) and the number of binding sites (n) of the static quenching process were further evaluated by the following equation (Lakowicz, Joseph R, 2000):

$$\log\frac{F_0-F}{F} = logK_a + n\,log[Q] \qquad (3)$$

where F_0 and F are fluorescence intensities of the complex without and with CGA, [Q] is the concentration of CGA. As listed in Table 1, the K_a values of lipase-CGA complexes were lower than those of LOX-CGA complexes at different temperatures. The decreased trend of K_a values of the temperature also show that the CGA which induced the quenching mechanism of two types of enzymes was static quenching. The values of n were approximately equal to 1, which demonstrate that there was only one class of binding site for CGA on two types of enzymes and the formation of complexes in intermolecular interactions at a molar ratio of 1:1. The values of K_a and n decreased with increasing temperature, which might have been caused

by the decomposition of enzyme-CGA complex.

3.3.2 Thermodynamic parameters

The Van't Hoff equation (Function 4) and Gibbs equation (Function 5) were used to calculate the thermodynamic parameters of interactions between small molecules and proteins (Ross & Subramanian, 1981):

$$lnK_a = -\frac{\Delta H}{RT} + \frac{\Delta S}{R} \quad (4)$$

$$\Delta G = \Delta H - T\Delta S \quad (5)$$

where K_a is the binding constant at different temperature T (298K, 304K, 310K); ΔH, ΔS and ΔG are the changes of enthalpy, entropy and free energy, respectively; R is the gas constant (8.314 J/mol·K).

The values of ΔH, ΔS and ΔG are presented in Table 1, the negative values of ΔH and ΔS show that the hydrogen bond and Van der Waals force interactions might play a major role during the binding process of both lipase-CGA and LOX-CGA systems (Ross & Subramanian, 1981). The negative values of ΔG suggest that the interactions between endogenous enzymes of fish flesh and CGA were spontaneous.

3.4 Synchronous fluorescence spectra analysis

The synchronous fluorescence spectroscopy is often used to analyze microenvironment changes surrounding amino acid fluorophore residues and study protein conformation changes. The $\Delta\lambda$ between emission wavelength and excitation wavelength established at 15 nm and 60 nm reflect the spectra features of Tyr and Trp, respectively.

As shown in Figs. 2c1, c2 and Figs. 2d1, d2, the synchronous fluorescence intensities of Tyr and Trp were both decreased following an increase in CGA. For $\Delta\lambda$=15 nm, a weak blue shift trend of maximum emission wavelength was observed with the gradual addition of CGA into the lipase solution (Fig. 2c1), but there was no shift observed for LOX (Fig. 2c2), which indicates that the interaction between lipase and

CGA slightly increased the hydrophobicity of microenvironment around Tyr residues (Peng, et al., 2016). For $\Delta\lambda$=60 nm, there was no obvious shift found in lipase (Fig. 2d1), a small red shift of maximum emission wavelength in LOX (Fig. 2d2) suggests that the addition of CGA slightly improved the polarity of the Trp residue microenvironment (Zhu, et al., 2017). The results imply that CGA may be closer to the Trp residue than Try residue in the LOX-CGA interaction, but it might not bind closer to neither Tyr nor Trp in lipase. According to the above results, there was no significant change in the enzymatic amino acid microenvironment. The changes in maximum emission wavelength with synchronous fluorescence are basically consistent with the results of former fluorescence quenching analysis.

3.5 UV-VIS spectroscopy analysis

UV-VIS absorption spectroscopy is a simple and useful method for investigating protein structural changes. The interactions of lipase/LOX, and CGA at different concentrations were studied using UV-VIS spectroscopy. As shown in Fig. 3a1 and Fig. 3a2, with the continuous increase in CGA concentration, the absorption peaks around 220 nm were gradually increased with a small blue shift indicating that CGA influenced the skeleton structures of these two types of endogenous enzymes (Farhadian, et al., 2019). The increased absorption intensity and red shift of peaks around 275 nm suggest the formation of complexes between enzymes and CGA. The absorbance of lipase-CGA and LOX-CGA complexes was significantly elevated with increasing concentrations between 250 nm and 350 nm. This implies that CGA could lead to the modification of polarity and hydrophilicity of microenvironment around aromatic amino acid residues of endogenous enzymes, which are responsible for changes of lipase and LOX conformation (Menezes, et al., 2019). Moreover, the shift of maximum emission wavelength and differences in UV spectra reconfirmed the fluorescence quenching of interactions between lipase/LOX and CGA was static quenching instead of dynamic quenching, which is similar former results presented in fluorescence quenching spectra (Zhu, et

al., 2017).

3.6 CD spectra analysis

The CD spectroscopy has been widely used to determine the changes in protein conformation. Different secondary structures of protein have different characteristic absorption bands in CD spectra. The fractions of α-helix, β-sheet, β-turn and random coil in lipase and LOX without or with CGA are presented in Table 2. Following an increase in CGA concentration, lipase's α-helix content decreased, while the contents of β-sheet and β-turn increased, and there was no apparent change observed in random coil content. Results support the notion that the binding of CGA and lipase might destroy the hydrogen and van der Waals' bonds in the secondary structure of lipase, which could lead to the extension of the spiral structure (Zhu, et al., 2018). The α-helix around the catalytic site of lipase stabilizes the enzyme, thus the loss of helical content might result in the destabilization of the structure of spatial protein (Su, et al., 2016).

On the other hand, the fractions of α-helix and β-sheet in the secondary structure of LOX increased, instead of decreasing in β-turn and random coil, which suggests that the secondary structure of LOX might be more firming after binding with CGA. The electrostatic interactions might have led to the increase in α-helix content (Shen, et al., 2019). The results described above indicate that the interactions with CGA affected the secondary structure of enzymes, and may have further hampered enzymatic catalytic sites and active centers, affecting the activity of enzymes (Peng, et al., 2016). The results are in accordance with the conclusion obtained from inhibitory effects of CGA on enzymatic activities in this study.

3.7 FT-IR spectra studies

The conformational changes of enzymes affected by CGA could also be investigated through FT-IR spectra. As shown in Fig. 3b1 and Fig. 3b2, the FT-IR spectra of free enzymes and enzyme-CGA complexes in the region of 4000-400 cm^{-1} were investigated. In spectroscopy of lipase-CGA complex (Fig. 3b1), the

342 peak (3229 cm^{-1}) might be associated with the N-H stretching vibration and the peak (2989 cm^{-1}) with
343 asymmetrical stretch of C-H (He, et al., 2018). The amide I (1700-1600 cm^{-1}) peak with the wavenumber at
344 1632cm^{-1} originated from C=O stretching vibration. The amide II (1600-1500 cm^{-1}) peaks which appeared
345 around 1550cm^{-1} resulted from C-N stretching and N-H bending vibrations (Zhu, et al., 2019). The
346 intensities of these peaks increased compared to those in free lipase.

347 In spectroscopy of the LOX-CGA complex (Fig. 3b2), there was a slight deviation and shift of the
348 amide A peak at 3446cm^{-1}, which originated mainly from the O-H stretching vibration and the N-H
349 stretching vibration, compared to LOX. The broader band at 2450cm^{-1} and the shift at 1138cm^{-1} might be
350 associated with intermolecular interactions. The intensities of peaks were slightly changed during the
351 interaction. The results confirm that interactions exist between CGA and enzymes, and hydrogen bonds are
352 the important force in complexes. The changes of spectra in amide I and amide II infrared absorption bands
353 suggest that CGA not only interacted with lipase and LOX, but also altered the secondary structures of
354 enzymes, which is consistent with results of CD spectra analysis.

355 **3.8 Particle size analysis**

356 The average particle sizes of enzyme-CGA complexes were investigated. Following the elevation of
357 CGA concentration, the average diameters of lipase increased from 1083±14 nm to 1314±18 nm (Fig. 3c1),
358 which confirm that the formation of lipase-CGA complex and CGA could cause the aggregation of lipase.
359 However, the average particle size of LOX only slightly increased from 149±1 nm to 155±1 nm (Fig.
360 3c2), which suggests that the complex might be formed between LOX and CGA, but the aggregation of the
361 enzyme was not obvious. The difference might be attributed to the different structures of lipase and LOX.
362 These phenomena are similar to those reported between wine polyphenols and yeast protein extract,
363 mannoproteins (Neguela, et al., 2016). The particle size distribution of enzyme-CGA complexes in Fig. 3d1

364 and Fig.3 d2 illustrates that lipase has a wider particle size distribution than LOX following the increase in
365 CGA concentration, which is consistent with former results (Zhu, et al., 2017).

366 **3.9 Molecular docking analysis**

367 Molecular docking is an effective and reliable computational technique for predicting possible binding
368 modes and studying ligand binding mechanisms of small molecules and protein. In this study, for the sake
369 of exploring deeper insight into the nature of the interactions between lipase/LOX and CGA theoretically,
370 the molecular docking method was used to analyze the binding process based on the CDOCKER protocol.

371 The docking interaction plots at the best active sites of enzymes are illustrated in Fig. 4a and Fig. 4b,
372 and the interaction details between the amino acid residues and CGA in different conditions from 3D
373 docking mode and 2D schematic diagram are demonstrated in Fig. 4c-d. It can clearly be seen that CGA
374 formed hydrogen bonds with lipase (Fig. 4c1), including conventional hydrogen bond with aspartic (Asp)
375 80 (Bond length-2.33 Å), carbon hydrogen bonds with catalytic residue serine (Ser) 153 (3.07 Å) and
376 arginine (Arg) 257 (2.86 Å), π-donor hydrogen bond with histidine (His) 264 (3.16 Å). Besides, hydrophobic
377 interactions between the benzene ring and Trp 253 (5.32 Å) near the acyl-binding pocket, weak interactions
378 such as Van Der Waals' force with surrounding amino acid residues are also presented in the interaction.
379 The results suggest that CGA was located close to Ser153 and His264 (Fig. 4d1), which were reported to be
380 amino acid residues near an enzyme active site (Martinez-Gonzalez, et al., 2017), and explained the
381 inhibitory effect of CGA on lipase activities. The result is in good agreement with the competitive type of
382 inhibition obtained from former lipase-CGA inhibition assay.

383 For the LOX-CGA complex, CGA formed more hydrogen bonds (Fig. 4c2 and 4d2), including
384 conventional hydrogen bonds with glutamic (Glu) 357 (Bond length-2.87 Å, 2.03 Å) and Arg 403 (2.87 Å,
385 2.47 Å), carbon hydrogen bond with Glu 357 (3.04 Å), Arg 403 (2.35 Å) and phenylalanine (Phe) 175 (2.48

386 Å). Hydrophobic interactions also exist between the benzene ring of CGA and Arg 403 (4.47 Å), isoleucine
387 (Ile) 400 (5.35 Å) and Ile 173 (5.37 Å). Miscellaneous interactions like metal-acceptor (3.09 Å) formed
388 between Fe and CGA. It can be deduced that hydrogen bonds, hydrophobic interactions and the Van Der
389 Waals' force are the dominant interactive forces that promote the binding of LOX and CGA, which further
390 validate or reconfirm the results of fluorescence spectra analysis.
391
392 **4 Conclusions**
393 The experimental results showed the inhibitory effect of CGA on endogenous lipase and LOX in grass carp
394 muscle, and the inhibition types were competitive inhibition and mixed inhibition respectively. In the study,
395 the interaction mechanisms between CGA and enzymes were also investigated using multi-spectroscopy
396 methods combined with molecular docking studies. These results indicated the formation of enzyme-CGA
397 complexes and changes in enzymatic conformation during binding reactions. The intrinsic fluorescence
398 intensities in two types of enzymes were significantly quenched with CGA mainly through static quenching.
399 The hydrophilic microenvironment and polar environment surrounding aromatic amino acid residues in
400 enzymes resulting from CGA were reflected in the shifts in fluorescence spectra and UV-Vis spectra. The
401 changes in the CD spectra and FT-IR spectra showed that CGA had different effects on secondary structures
402 of lipase and LOX. The addition of CGA resulted in the aggregation of lipase as demonstrated from the
403 results of particle size analysis. Molecular docking analysis suggested that CGA may bind close to the active
404 site of lipase. Hydrogen bonds, hydrophobic interactions and the Van Der Waals' force were the main
405 interactions. The interactions between CGA and enzymes may provide a better understanding of the
406 inhibitory mechanism of CGA during the period of preservation, and in favor of its application in aquatic
407 products. This study could provide basic mechanisms of the inhibitory effects of polyphenols on lipid

oxidation during food preservation.

Acknowledgement This study was supported by the Nature Science Foundation of China (No. 31772047), the Fundamental Research Funds for the Central universities (No. 2662019PY031 and 2662018JC056) and the China Agriculture Research System (CARS-45-27).

Authorship contribution statement

Qiongju Cao: Methodology, Formal analysis, Writing - original draft. **Yuan Huang**: Methodology, Formal analysis. **Quan-Fei Zhu**: Formal analysis; **Mingwei Song**: Conceptualization, Funding acquisition. **Shanbai Xiong**: Academic instructor, Project administration. **Anne Manyande**: Writing - review & editing. **Hongying Du**: Supervision，Conceptualization, Formal analysis, Funding acquisition, Writing - review & editing.

Conflict of interest: The authors report no conflict of interest.

Reference

Andreou, A., Göbel, C., Hamberg, M., & Feussner, I. (2010). A bisallylic mini-lipoxygenase from cyanobacterium Cyanothece sp. that has an iron as cofactor. *Journal of Biological Chemistry, 285*, 14178–14186.

Banerjee, S. (2006). Inhibition of mackerel (Scomber scombrus) muscle lipoxygenase by green tea polyphenols. *Food Research International, 39*(4), 486-491.

Cao, Q., Du, H., Huang, Y., Hu, Y., You, J., Liu, R., Xiong, S., & Manyande, A. (2019). The inhibitory effect of chlorogenic acid on lipid oxidation of grass carp (Ctenopharyngodon idellus) during chilled storage. *Food and Bioprocess Technology, 12*(2019), 2050–2061.

Chauhan, P., Das, A. K., Nanda, P. K., Kumbhar, V., & Yadav, J. P. (2018). Effects of nigella sativa seed extract on lipid and protein oxidation in raw ground pork during refrigerated storage. *Nutrition & Food Science, 48*(1), 2-15.

Cherif, S., & Gargouri, Y. (2009). Thermoactivity and effects of organic solvents on digestive lipase from hepatopancreas of the green crab *Food Chemistry, 116*(1), 82-86.

Cysewski, P. (2008). A post-SCF complete basis set study on the recognition patterns of uracil and cytosine by aromatic and π–aromatic stacking interactions with amino acid residues. *Physical Chemistry Chemical Physics, 10*, 2636–2645.

Farhadian, S., Shareghi, B., Asgharzadeh, S., Rajabi, M., & Asadi, H. (2019). Structural characterization of α-chymotrypsin after binding to curcumin: Spectroscopic and computational analysis of their binding

mechanism. *Journal of Molecular Liquids, 289*, 111111.
Gata, J. L., Pinto, M. C., & Macias, P. (1996). Lipoxygenase activity in pig muscle: purification and partial characterization. *Journal of Agricultural and Food Chemistry, 44*(9), 2573-2577.
Ge, Y., Li, Y., Wu, T., Bai, Y., Yuan, C., Chen, S., Gakushic, I., & Hu, Y. (2020). The preservation effect of CGA-Gel combined with partial freezing on sword prawn (Parapenaeopsis hardwickii). *Food Chemistry, 313*, 126078.
Gugliucci, A., Bastos, D. H. M., Schulze, J., & Souza, M. F. F. (2009). Caffeic and chlorogenic acids in Ilex paraguariensis extracts are the main inhibitors of AGE generation by methylglyoxal in model proteins. *Fitoterapia, 80*(6), 339-344.
He, W., Mu, H., Liu, Z., Lu, M., Hang, F., Chen, J., Zeng, M., Qin, F., & He, Z. (2018). Effect of preheat treatment of milk proteins on their interactions with cyanidin-3-O-glucoside. *Food Research International, 107*, 394-405.
Huang, X., & Ahn, D. U. (2019). Lipid oxidation and its implications to meat quality and human health. *Food Science and Biotechnology, 28*, 1275-1285.
Huo, Y., Du, H., Xue, B., Niu, M., & Zhao, S. (2016). Cadmium Removal from Rice by Separating and Washing Protein Isolate. *J Food Sci, 81*(6), T1576-T1584.
Jiao, W., Shu, C., Li, X., Cao, J., Fan, X., & Jiang, W. (2019). Preparation of a chitosan-chlorogenic acid conjugate and its application as edible coating in postharvest preservation of peach fruit. *Postharvest Biology and Technology, 154*, 129-136.
Ju, J., Liao, L., Qiao, Y., Xiong, G., Li, D., & Wang, C. (2018). The effects of vacuum package combined with tea polyphenols (v+tp) treatment on quality enhancement of weever (micropterus salmoides) stored at 0℃ and 4℃. *LWT-Food Science and Technology, 91*, 484-490.
Karar, M. G. E., Matei, M.-F., Jaiswal, R., Illenberger, S., & Kuhnert, N. (2016). Neuraminidase inhibition of dietary chlorogenic acids and derivatives-potential antivirals from dietary sources. *Food and Function, 7*(4), 2052-2059.
Kuepethkaew, S., Sangkharak, K., Benjakul, S., & Klomklao, S. (2017). Use of TPP and ATPS for partitioning and recovery of lipase from Pacific white shrimp(Litopenaeus vannamei) hepatopancreas. *Journal of Food Science and Technology, 54*(12), 3880-3891.
Lakowicz, J. R. (2000). On Spectral Relaxation in Proteins. *Photochemistry and Photobiology, 72*(4), 421-437.
Lakowicz, J. R. (2006). Quenching of Fluorescence. *Principles of Fluorescence Spectroscopy*, 227-230.
Lowry, O. H., Rosebrough, N. J., Farr, A. L., & Randall, R. J. (1951). Protein Measurement with the Folin Phenol Reagent. *Journal of Biological Chemistry, 193*(1), 265-275.
Martinez-Gonzalez, A. I., Alvarez-Parrilla, E., Díaz-Sánchez, Á. G., Rosa, L. A. d. l., Núñez-Gastélum, J. A., Vazquez-Flores, A. A., & Gonzalez-Aguilar, G. A. (2017). *In vitro* inhibition of pancreatic lipase by polyphenols: a kinetic, fluorescence spectroscopy and molecular docking study. *Food Technology and Biotechnology, 55*(4), 519-530.
Menezes, T. M., Almeida, S. M. V., Moura, R. O., Seabra, G., Lima, M. C. A., & Neves, J. L. (2019). Spiro-acridine inhibiting tyrosinase enzyme Kinetic, protein-ligand interaction and molecular docking studies. *International Journal of Biological Macromolecules, 122*(2019), 289–297.
Neguela, J. M., Poncet-Legrand, C., Sieczkowski, N., & Vernhet, A. (2016). Interactions of grape tannins and wine polyphenols with a yeast protein extract, mannoproteins and β-glucan. *Food Chemistry, 210*(1), 671-682.
Nikpour, M., Mousavian, M., Davoodnejad, M., & Sadeghian, M. A. (2013). Synthesis of new series of pyrimido[4,5-b][1,4] benzothiazines as 15-lipoxygenase inhibitors and study of their inhibitory

mechanism. *Medicinal Chemistry Research, 22*(10), 5036-5043.
Olthof, M. R., Hollman, P. C. H., & Katan, M. B. (2001). Chlorogenic Acid and Caffeic Acid Are Absorbed in Humans. *The Journal of Nutrition, 131*(1), 66-71.
Peng, X., Zhang, G., Liao, Y., & Gong, D. (2016). Inhibitory kinetics and mechanism of kaempferol on α-glucosidase. *Food Chemistry, 190*, 207-215.
Ross, P. D., & Subramanian, S. (1981). Thermodynamics of protein association reactions: forces contributing to stability. *Biochemistry, 20*(11), 3096-3102.
Schreiber, R., Xie, H., & Schweiger, M. (2019). Of mice and men: The physiological role of adipose triglyceride lipase (ATGL). *BBA-Molecular and Cell Biology of Lipids, 1864*(6), 880-899.
Shen, H., Zhao, M., & Sun, W. (2019). Effect of pH on the interaction of porcine myofibrillar proteins with pyrazine compounds. *Food Chemistry, 287*(2019), 93-99.
Shi, J., Lei, Y., Shen, H., Hong, H., Yu, X., Zhu, B., & Luo, Y. (2019). Effect of glazing and rosemary (Rosmarinus officinalis) extract on preservation of mud shrimp (Solenocera melantho) during frozen storage. *Food Chemistry, 272*(30), 604-612.
Smichi, N., Gargouri, Y., Miled, N., & Fendri, A. (2013). A grey mullet enzyme displaying both lipase and phospholipase activities Purification and characterization. *International Journal of Biological Macromolecules, 58*, 87-94.
Sreeparna, B. (2006). Inhibition of mackerel (Scomber scombrus) muscle lipoxygenase by green tea polyphenols. *Food Research International, 39*(2006), 486–491.
Su, J., Wang, H., Ma, C., Liu, C., Rahman, M. T., Gao, C., & Nie, R. (2016). Hypolipidemic mechanism of gypenosides via inhibition of pancreatic lipase and reduction in cholesterol micellar solubility. *European Food Research and Technology, 242*(3), 305-312.
Sun, Z., Zhang, X., Wu, H., Wang, H., Bian, H., Zhu, Y., Xu, W., Liu, F., Wang, D., & Fu, L. (2020). Antibacterial activity and action mode of chlorogenic acid against Salmonella Enteritidis, a foodborne pathogen in chilled fresh chicken. *World Journal of Microbiology and Biotechnology, 36*, 24.
Utrera, M., Morcuende, D., Ganhão, R., & Estévez, M. (2015). Role of Phenolics Extracting from Rosa canina L. on Meat Protein Oxidation During Frozen Storage and Beef Patties Processing. *Food and Bioprocess Technology, 88*(3), 854–864.
Xiong, G., Gao, X., Wang, P., Xu, X., & Zhou, G. (2016). Comparative study of extraction efficiency and composition of protein recovered from chicken liver by acid-alkaline treatment. *Process Biochemistry, 51*, 1629-1635.
Xu, J., Hao, M., Sun, Q., & Tang, L. (2019). Comparative studies of interaction of β-lactoglobulin with three polyphenols. *International Journal of Biological Macromolecules, 136*, 804-812.
Ying, M., Meti, M. D., Xu, H., Wang, Y., Lin, J., Wu, Z., Han, Q., Xu, X., He, Z., Hong, W., & Hu, Z. (2018). Binding mechanism of lipase to Ligupurpuroside B extracted from Ku-Ding tea as studied by multi-spectroscopic and molecular docking methods. *International Journal of Biological Macromolecules, 120*(2018), 1345–1352.
Yu, Q., Fan, L., & Duan, Z. (2019). Five individual polyphenols as tyrosinase inhibitors: Inhibitory activity, synergistic effect, action mechanism, and molecular docking. *Food Chemistry, 297*(2019), 124910-124920.
Zhu, J., Sun, X., Wang, S., Xu, Y., & Wang, D. (2017). Formation of nanocomplexes comprising whey proteins and fucoxanthin: Characterization, spectroscopic analysis, and molecular docking. *Food Hydrocolloids, 63*, 391-403.
Zhu, M., Wang, L., Wang, Y., Zhou, J., Ding, J., Li, W., Xin, Y., Fan, S., Wang, Z., & Wang, Y. (2018).

529 Biointeractions of Herbicide Atrazine with Human Serum Albumin: UV-Vis, Fluorescence and Circular
530 Dichroism Approaches. *International Journal of Environmental Research and Public Health, 15*, 116.
531 Zhu, S., Yuan, Q., Yang, M., You, J., Yin, T., Hu, Y., & Xiong, S. (2019). A quantitative comparable study on
532 multi-hierarchy conformation of acid and pepsin-solubilized collagens from the skin of grass carp
533 (*Ctenopharyngodon idella*). *Materials Science & Engineering C, 96*(2019), 446-457.
534
535

536 **Table 1.** Quenching constants (K_{SV}), binding constants (K_a) and thermodynamic parameters of enzymes-

537 CGA under different temperatures

	T (K)	K_{sv} (10^4 L/mol)	K_q (10^{12} L/mol·s)	R_a^2	K_a (10^5 L/mol)	n	R^2	ΔH (KJ/mol)	ΔS (J/mol·K)	ΔG (KJ/mol)
	298	2.11	2.11	0.990	0.33	1.05	0.998			-25.68
Lipase	304	1.67	1.67	0.997	0.16	0.99	0.996	-97.57	-241.23	-24.48
	310	1.55	1.55	0.995	0.07	0.92	0.995			-22.78
	298	3.94	3.94	0.996	2.06	1.17	0.999			-30.56
LOX	304	3.75	3.75	0.994	1.75	1.15	0.998	-63.76	-111.42	-30.00
	310	3.04	3.04	0.993	0.78	1.10	0.998			-29.22

538

539

540

Table 2 Conformation changes in secondary structures of enzymes under difference treatments of CGA.

	Concentration of CGA (10^{-6} mol·L^{-1})	Secondary structure (%)			
		α-Helix	β-Sheet	β-Turn	Random coil
lipase	0	43.17	25.17	5.93	25.67
	20	41.05	27.40	6.50	25.00
	40	38.53	26.15	8.73	26.53
LOX	0	43.70	20.00	12.00	24.30
	20	44.03	23.73	9.03	23.17
	40	46.40	23.97	7.80	23.30

Figures/Tables Legends

Fig. 1 Results of purity of enzymes (SDS-PAGE) and inhibitory activities of lipase and LOX. *Note:* ***a)*** *1 and 4-Markers; 2-Crude enzyme sample; 3-LOX; 5-Lipase;* ***b)*** *Inhibitory ratios of lipase (**b1**: c_{lipase}=0.1 mg/mL; $c_{4\text{-}npb}$=3.0 mM) and LOX (**b2**: c_{LOX}=0.1mg/mL; $c_{linoleic\ acid}$=20.0mM);* ***c)*** *Inhibitory types of lipase (**c1**: $c_{4\text{-}npb}$= 3.0 mM; c_{CGA}= 0.0-0.3 mg/mL) and LOX (**c2**: $c_{linoleic\ acid}$= 15.0mM; c_{CGA}= 0.0-0.2 mg/mL).* ***d)*** *Inhibitory kinetics of lipase (**d1**: c_{lipase} = 0.1 mg/mL; $c_{4\text{-}npb}$ = 1.0-5.0 mM; c_{CGA} = 0.0-0.3 mg/mL) and LOX (**d2**: c_{LOX} = 0.1 mg/mL; $c_{linoleic\ acid}$= 5.0-25.0 mM; c_{CGA}= 0.0-0.2 mg/mL)*

Fig. 2. Fluorescence spectra analysis of the interaction between CGA and ligase (a1-d1) or LOX (a2-d2). *Note: Figure legends: c_{CGA}= 0.0, 5.0, 10.0, 15.0, 20.0, 25.0, 30.0, 35.0, 40.0×10^{-6} mol/L; a) Fluorescence spectra (T=298K); b) Stern-Volmer plots for fluorescence quenching; c and d) Synchronous fluorescence spectrum of lipase and LOX, c-Δλ=15 nm, d-Δλ=60 nm*.

Fig. 3. UV-VIS/FT-IR spectra and particle size analysis of ligase (a1-d1) or LOX (a2-d2) after the interaction of CGA. *Note: Figure legends: c_{CGA}=×10^{-6} mol/L; a) UV–VIS absorption*; *b) FT-IR spectra; c) Distribution of average particle size; d) Intensity of particle size distribution.*

Fig. 4. Molecular docking analysis of the interaction of CGA and ligase (a1-d1) or LDX (a2-d2). *Note: a) and b): Docking ligand in the binding site; c) Results of 3D molecular docking modeling; d) Results of 2D molecular docking modeling.*

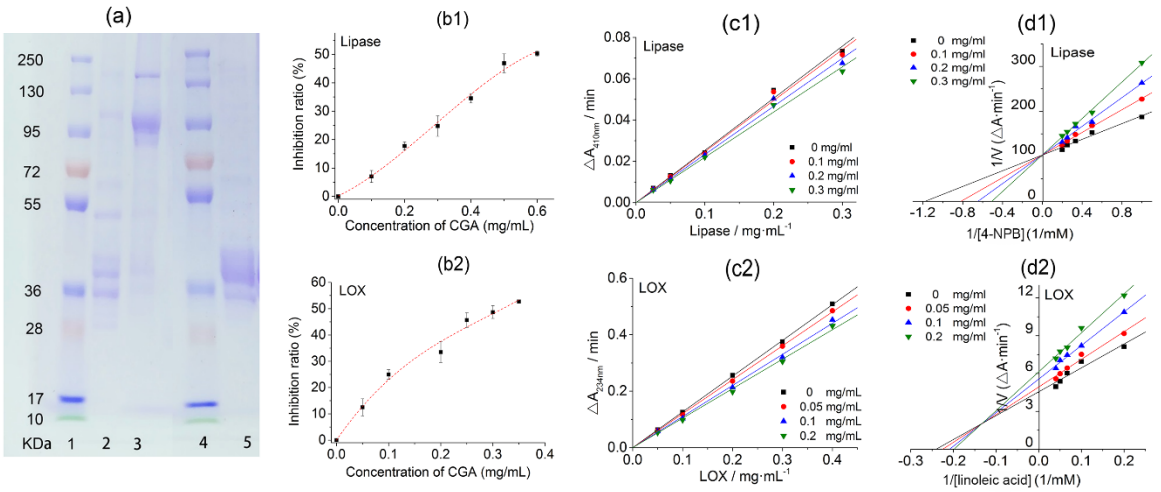

563

564 **Fig. 1** Results of purity of enzymes (SDS-PAGE) and inhibitory activities of lipase and LOX. *Note:* ***a)*** *1*

565 *and 4-Markers; 2-Crude enzyme sample; 3-LOX; 5-Lipase;* ***b)*** *Inhibitory ratios of lipase (****b1****:* c_{lipase}*=0.1*

566 *mg/mL;* $c_{4\text{-}npb}$*=3.0 mM) and LOX (****b2****:* c_{LOX}*=0.1mg/mL;* $c_{linoleic\ acid}$*=20.0mM);* ***c)*** *Inhibitory types of lipase*

567 *(****c1****:* $c_{4\text{-}npb}$*= 3.0 mM;* c_{CGA}*= 0.0-0.3 mg/mL) and LOX (****c2****:* $c_{linoleic\ acid}$*= 15.0mM;* c_{CGA}*= 0.0-0.2 mg/mL).*

568 ***d)*** *Inhibitory kinetics of lipase (****d1****:* c_{lipase} *= 0.1 mg/mL;* $c_{4\text{-}npb}$ *= 1.0-5.0 mM;* c_{CGA} *= 0.0-0.3 mg/mL) and*

569 *LOX (****d2****:* c_{LOX} *= 0.1 mg/mL;* $c_{linoleic\ acid}$*= 5.0-25.0 mM;* c_{CGA}*= 0.0-0.2 mg/mL)*

570

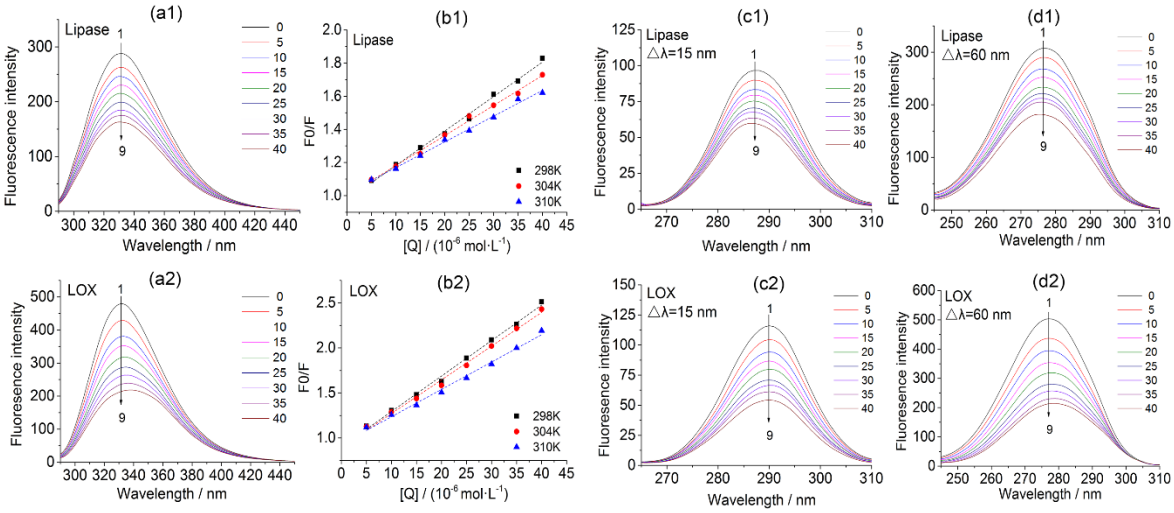

Fig. 2. Fluorescence spectra analysis of the interaction between CGA and ligase (a1-d1) or LOX (a2-d2).

Note: Figure legends: c_{CGA}= 0.0, 5.0, 10.0, 15.0, 20.0, 25.0, 30.0, 35.0, 40.0×10^{-6} mol/L; a) Fluorescence spectra (T=298K); b) Stern-Volmer plots for fluorescence quenching; c and d) Synchronous fluorescence spectrum of lipase and LOX, c-Δλ=15 nm, d-Δλ=60 nm.

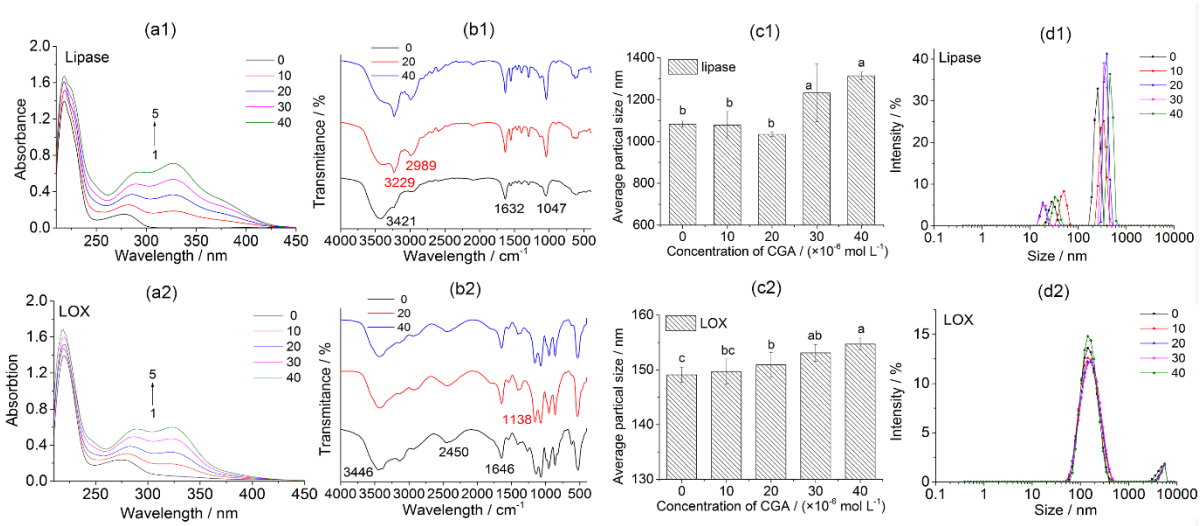

Fig. 3. UV-VIS/FT-IR spectra and particle size analysis of ligase (a1-d1) or LOX (a2-d2) after the interaction of CGA. *Note: Figure legends:* c_{CGA}*=×10*$^{-6}$ *mol/L; a) UV–VIS absorption*; *b) FT-IR spectra; c) Distribution of average particle size; d) Intensity of particle size distribution.*

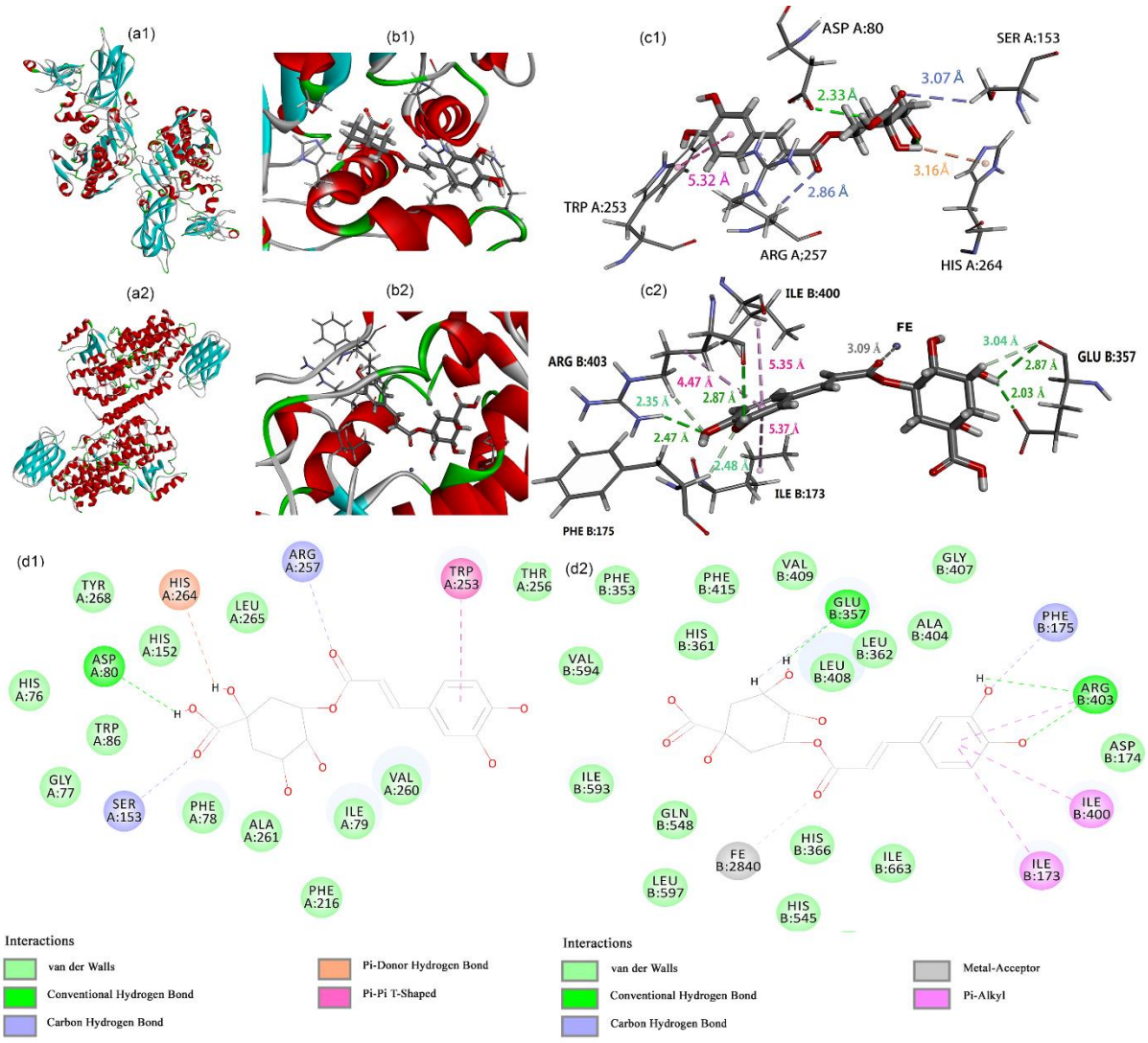

Fig. 4. Molecular docking analysis of the interaction of CGA and ligase (a1-d1) or LDX (a2-d2). *Note: a) and b): Docking ligand in the binding site; c) Results of 3D molecular docking modeling; d) Results of 2D molecular docking modeling.*